Int J Cardiovasc Imaging (2009) 25:217–230
DOI 10.1007/s10554-009-9439-0

ORIGINAL PAPER

Low-dose prospectively gated 256-slice coronary computed tomographic angiography

Wm. Guy Weigold · Mark E. Olszewski · Matthew J. Walker

Received: 11 December 2008 / Accepted: 4 February 2009 / Published online: 12 March 2009

Abstract Since the introduction of 64-slice scanners, multidetector computed tomography (MDCT) has experienced a marked increase in adoption for the noninvasive assessment of coronary artery disease, although radiation dose concerns remain. The recent introduction of prospective coronary CT angiography (CCTA) has begun to address these concerns; however, its applicability with existing scanners remains limited to cohorts defined by heart rate, heart rate variability, and body mass index. This paper reviews prospective CCTA, the effect of heart rate and heart rate variability on image quality, and the physiologic basis for selection of optimal prospective imaging windows. We then discuss 256-slice technology and our first 4 months of clinical experience with 256-slice prospective CCTA. Our early clinical results indicate that high-quality, low-dose prospective coronary CTA may be applied to patients with higher heart rates, higher BMI, and with less sensitivity to heart rate variability using 256-slice MDCT.

Keywords 256-Slice MDCT · Prospective gating · Radiation exposure · Radiation reduction · Coronary CT angiography · Step-and-shoot · Low dose

Wm. G. Weigold (✉)
Department of Medicine (Cardiology), Cardiovascular Research Institute, Washington Hospital Center, 110 Irving Street, NW, Suite 4B-1, Washington, DC 20010, USA
e-mail: guy.weigold@medstar.net

M. E. Olszewski · M. J. Walker
Computed Tomography Clinical Science, Philips Healthcare, 595 Miner Road, Cleveland, OH44143, USA

M. E. Olszewski
e-mail: mark.olszewski@philips.com

M. J. Walker
e-mail: matthew.walker@philips.com

Introduction

The past five years have seen tremendous growth in the use of multidetector computed tomography (MDCT) for the noninvasive detection and evaluation of coronary artery disease. Still, safety concerns regarding radiation dose, intravenous contrast, and β blocker medications remain barriers to more widespread adoption and reimbursement of coronary CT angiography (CCTA) using the standard retrospectively gated helical technique [1–5].

A number of technological advances have attempted to address radiation dose concerns [6]. Among these, electrocardiogram (ECG) triggered tube current modulation [7], tube voltage reduction [8], adaptive tube current selection, and patient-specific scan protocol algorithms [9, 10] have reduced the effective radiation dose associated with retrospective CCTA. While these advances have resulted in dose reductions of 35–65%, retrospective CCTA effective doses are still reported in the range of 14–21 mSv [11, 12]. Consequently, further

dose reductions are necessary to facilitate more widespread adoption of CCTA.

A significant step forward in radiation dose reduction is now being realized with technological advances that enable the use of prospectively gated axial coronary CTA. Using 64-slice and dual-source MDCT, prospective CCTA has been shown to be technically [13] and clinically feasible [14–21]. These initial studies have demonstrated the potential for prospective CCTA to substantially reduce the effective radiation dose delivered during CCTA and have reported dose reductions of 52–85% [15, 22], with mean effective doses from 2.1 to 6.2 mSv [17, 20].

Despite the promise of prospective CCTA shown by these early studies, current 64-slice and dual-source prospective CCTA is limited to patients with heart rates below 63 [17] and 75 bpm [16, 20]. These studies also note challenges with respect to predictive ECG triggering in patients with heart rate variations [15, 23]. Additionally, 64-slice and dual-source prospective CCTA have not been studied extensively in obese and bariatric populations. Lastly, intravenous contrast and β blocker medications remain a concern for all coronary angiographic procedures [1]. Thus, while the advent of prospective CCTA holds promise as a powerful means of radiation dose reduction, limitations when applied via 64-slice and dual-source scanners may restrict the application of this low-dose imaging method to a narrow range of select patients.

This paper will review prospective CCTA, examine the effect of heart rate and heart rate variability on image quality, discuss the physiologic basis for selection of optimal prospective imaging windows, and show how wide-area detector (256-slice and greater) MDCT addresses the aforementioned limits and enables the application of low-dose prospective CCTA in a wider range of patients. We will then present a brief report of our initial clinical experience with a particular 256-slice MDCT system (Brilliance iCT, Philips Healthcare, Cleveland, OH, USA).

Prospectively gated axial coronary CTA literature review

Early clinical studies have demonstrated prospective CCTA techniques enable imaging with a 52–85% lower effective dose [15, 22] than retrospective coronary CTA with equivalent [16, 18, 20] or improved [14] image quality (IQ) compared to retrospective CCTA, resulting in 95.0–99.8% assessable segments [17, 22], when reported. With prospective CCTA, mean effective radiation dose ranged from 2.1 to 6.2 mSv [17, 20], with a minimum effective dose of 0.75 mSv [14] and a maximum effective dose of 11.9 mSv [20].

The patient cohorts examined with prospective CCTA in these early studies demonstrated mean heart rates (HR) of 56.0–60.0 beats per minute (bpm) [18, 22], with a minimum of 35.8 and a maximum of 73.0 bpm, when reported [16, 21]. To achieve the reported heart rates, 13–100% of patients were administered oral and/or intravenous β blocker medication prior to examination or were receiving β blockers as part of medical therapy [17, 21]. Heart rate variation (HRV) during the CCTA acquisition was only reported in two studies and ranged from 0.2 to 11.0 bpm [17, 21]. Only one study reported the capability to manage ectopic beats, such as premature atrial contractions (PAC) or premature ventricular contractions (PVC), during prospective acquisitions; however no data were presented to support this capability [18]. These studies documented a minimum and maximum body mass index (BMI) of 14.6 [14] and 54.1 [22] kg/m^2, respectively; however, the mean BMI varied little across the studied populations from 24.5 to 29.6 kg/m^2 [21, 22], as reported in all but one study.

Scan protocols of these early prospective CCTA studies reported craniocaudal coverage, number of axial acquisitions, and associated scan durations. Reported coverage ranged from 96.0 to 279 mm [20, 21], with the second longest coverage reported as 175.0 mm [14]. Based on available detector collimations of 19.2 mm [15, 19, 21], 40.0 mm [14, 16–18, 20], and 160.0 mm [22], the number of axial acquisitions—or shots—required to achieve the craniocaudal coverage varied from 1 to 8 [21, 22], with the minimum and maximum number of shots associated with the largest and smallest detector collimation, respectively. The combination of detector collimations and coverage resulted in mean scan durations of 4.2–15.4 s [14, 19]. While not reported, the scan times of single axial acquisitions were likely less than the gantry rotation time of 0.35 s in some cases, depending on HR and duration of X-ray on time. Transaxial field

of view (FOV) was only reported in three studies and varied from 180 [21] to 250 mm [14, 18]. Given the increased overlap requirements associated with the cone beam geometry of a 40.0 mm detector collimation and a FOV greater than 250 mm [13], the reported FOV in the remaining studies was likely less than 250 mm for all patients.

Based on these reported scan durations, contrast administration in the prospective CCTA studies documented typical bolus volumes of 41–105 ml per patient [20, 21], noting that the smallest contrast boluses were associated with tube voltage of 100 kVp, rather than the standard 120 kVp due to improved conspicuity of iodinated contrast at lower energies [24]. As expected, the prospective CCTA literature supports a trend of smaller contrast volumes associated with shorter scan durations, as evidenced by Earls et al. and Hirai et al. who reported mean scan durations of 4.2 and 5.6 s with minimum contrast volumes of 50 and 56 ml, respectively [14, 16]. Conversely, the maximum contrast volume of 103 ml used by Stolzmann et al. was from a cohort with a mean scan time of 14.4 s from an 8-shot acquisition [21].

All studies used a prospective ECG trigger in mid-diastole, typically at 70% [15, 19–21] or 75% [14, 16–18, 22] of the R-R interval. To achieve the reported dose reductions, the X-ray acquisition duration at the mid-diastolic trigger resulted in a single reconstructed phase in most studies; however, some studies reported the use of ±100 ms [14] or more [22] padding to reconstruct additional phases around the mid-diastolic trigger point, for example between 65% and 85% of the R-R interval. No study reported prospective triggering at an end-systolic rest phase, regardless of HR. Furthermore, reconstructed phases at both end-diastole and end-systole necessary for functional analysis (e.g., ejection fraction) were not acquired during the same exam using prospective CCTA in any study.

It is important to note that while prospective CCTA confers a significant reduction in effective radiation dose and provides equivalent or improved image quality relative to retrospective techniques, the literature highlights some important limitations to the applicability of current 64-slice and dual-source MDCT with respect to HR, HRV, and BMI. Maximum HR thresholds of 63 [17]–75 bpm [16, 20] were reported for prospective imaging, with Stolzmann et al. reporting a threshold of less than 59.9 bpm for predicting motion artifacts via receiver operating characteristic (ROC) curve (AUC = 0.818) [21]. Similarly, Gutstein et al. reported that a HR greater than 70 bpm, HRV greater than 10 bpm, and a BMI greater than 30 kg/m^2 all predict lower image quality [15]. Stolzmann et al. substantiate this BMI limit of 30 kg/m^2 [21]. Furthermore, Husmann et al. reported IQ was inversely related to HR and BMI with 98.9% segments assessable at heart rates less than 63 bpm and only 85.2% assessable at heart rates greater than or equal to 63 bpm [17]. With respect to HRV, Husmann et al. reported that image quality was not related to HRV; however the mean reported HRV in this study was only 1.5 bpm [17]. Alternatively, ROC analysis by Stolzmann et al. reported HRV had a significant effect on stair-step artifact (AUC = 0.79), with a maximum HRV of 11.0 bpm [21], likely attributed to the long scan durations or number of shots. Likewise, a steep rise in HR may occur during long duration scans and result in severe IQ deterioration, as noted by Scheffel et al. [19]. Lastly, it is important to note that long scan durations increase the opportunity for ectopic beats.

As noted, the existing 64-slice and dual-source MDCT technology limit the HR and HRV that permit high image quality prospective CCTA examinations. Therefore, to apply this technology to a wider patient population, heart rates must fall within the previously noted ranges. In particular, a large cohort study by Earls et al. noted that greater than 40% of all patients presenting for CCTA would have to be excluded from prospective CCTA without pharmacological heart rate control [23]. Despite HR control, including multiple oral and/or intravenous doses of β blocker or calcium channel blockers in approximately 7% of patients, Earls et al. noted that 9.5% of patients still failed to meet appropriate prospective HR or HRV threshold [23].

In summary, early evidence suggests that prospective CCTA using 64-slice [14, 16–18, 20] and dual-source [15, 19, 21] MDCT—although an effective dose reduction technique—remains limited to patient cohorts strictly defined by heart rate, heart rate variability, and body mass index. More specifically, HR greater than 70 bpm, HRV greater than 10 bpm, and BMI greater than 30 kg/m^2 all predict lower image quality. In this way, structured clinical algorithms are necessary to appropriately select patients for prospective CCTA.

Implications of cardiac physiology for prospective coronary imaging

From a physiological point of view, the heart has two quiescent periods: one during mid-diastole and one at end-systole. Mid-diastole, or diastasis, is the period of slow ventricular filling occurring just prior to atrial systole and represents a relatively long duration within the cardiac cycle without myocardial motion. The quiescent period at end-systole is a composite of three different phases of the cardiac cycle: reduced or absent ejection, protodiastole, and isovolumetric relaxation [25–27]. Reduced ejection is defined as the phase where the ventricular pressure falls below that of the outflow tract, resulting in decreased ventricular emptying [26, 27]. Protodiastole represents the time between the end of ventricular contraction and aortic valve closure [27]. The isovolumetric relaxation time (IVRT) begins with the closing of the aortic and pulmonary (semilunar) valves and opening of the mitral and tricuspid (atrioventricular) valves [27, 28]. These three consecutive phases—reduced ejection phase, protodiastole and IVRT—each exhibit minimal to no myocardial motion and their combined duration results in a relatively long end-systolic rest period [25, 27, 28].

Despite the quiescent nature of these end-diastolic and end-systolic periods, their durations vary with heart rate. The end-diastolic rest period varies significantly with HR and exhibits a curvilinear shortening as HR increases [27–29]. Across the normal physiologic range of heart rates, typical diastasis durations vary from approximately 350–600 ms at 40 bpm [29, 30] to approximately 90–150 ms at 70 bpm [29–31]. It is important to note that at heart rates above 80 bpm, diastasis is completely absent [29].

In contrast, the end-systolic rest period remains relatively constant with increasing heart rate, but does exhibit a minor linear shortening as heart rate increases [27, 28, 32, 33]. Mean (±SD) protodiastole and IVRT durations of 29 ± 12 (range, 0–55) and 62 ± 14 (range, 31–91) have been reported [32]. Furthermore, IVRT typically varies from 117 to 93 ms at 40 and 100 bpm, respectively [34]. Given the total electromechanical systolic duration of approximately 450–335 ms at 40 and 100 bpm, respectively [32–34], the composite duration of end-systolic rest period can range from approximately 100–230 ms, depending on heart rate.

The mid-diastolic and end-systolic rest periods provide two opportunities to image the coronary arteries with MDCT. As noted above, a mid-diastolic rest period is physiologically suited for imaging at heart rates below 75 bpm; however, at higher heart rates, this imaging window becomes prohibitively short, and end-systolic imaging is physiologically necessary given MDCT single cycle temporal resolutions. Current 64-slice and dual-source MDCT single cycle temporal resolutions range from 83 to 210 ms, but adaptive multicycle reconstruction may be used to improve temporal resolution for retrospective scans [35]. Such multicycle reconstruction methods may be variably employed with prospective CCTA depending on the scanner manufacturer. Multicycle reconstruction cannot be employed when data from a single cardiac cycle are acquired. In this case, the temporal resolution is limited to the native single cycle temporal resolution of the scanner. Consequently, the interaction between the single cycle temporal resolution of current generation MDCT scanners and the heart rate-dependent mid-diastolic and end-systolic rest period is important. This is supported by the mid-diastolic triggering and HR threshold of 70 bpm reported in the existing prospective CCTA literature. Moreover, depending on the duration of the CCTA examination, HRV can cause these rest periods to vary in location and duration between adjacent cardiac cycles, thus supporting a limit of 10 bpm for HRV [15, 23].

Additionally, accurate, on-the-fly prediction of cardiomechanical rest periods is crucial to satisfactory prospective imaging. Unlike retrospective imaging, in which reconstruction windows can be repositioned after the exam, single-phase acquisitions using prospective triggering require accurate prediction of rest periods with minimal motion. Use of the electrocardiogram (ECG) to predict the cardiomechanical rest state is possible when the cardiac rhythm is monotonous and the HR varies minimally, but breaks down when ectopy occurs or the HR changes dramatically. The acquisition of extra data around a predicted imaging window—so-called "padding"—allows for some retrospective flexibility in reconstruction window adjustment [14, 36]. In addition to optimally centering the imaging window within the expected rest period, it is necessary to physiologically align these imaging windows at the same cardiomechanical state to minimize the conspicuity of stair-step artifacts in

reconstructed image volumes from acquisitions requiring more than one axial shot to cover the desired craniocaudal anatomy. Such stair-step artifacts can be attributed to prediction errors associated with either poor QRS complex detection and/or heart rate variability. Consequently, these artifacts will likely be more pronounced in patients with challenging ECGs and/or scans of long duration. It is also important to note the relatively long duration of mid-diastolic rest periods at low heart rates facilitates easier prospective prediction and alignment of appropriate imaging windows. Yet, at higher heart rates, these tasks become easier in end-systole.

Prospectively gated axial coronary CTA using 256-slice MDCT

In light of the aforementioned limitations of 64-slice and dual-source MDCT for prospectively gated axial coronary CTA, further technical advances are necessary to image patients with less sensitivity to heart rate variability and over a wider range of heart rates and BMI. The advent of next generation MDCT with faster gantry rotation times, increased X-ray tube power, and larger detector coverage may facilitate the application of prospective CCTA imaging in this wider population. Recently, a 256-slice MDCT scanner with 0.27 s rotation, 120 kW X-ray tube and generator, and an 80.0 mm detector array has been introduced (Brilliance iCT, Philips Healthcare, Cleveland, OH, USA). This system potentially enables imaging beyond the 70 bpm HR and 30 kg/m^2 BMI thresholds with less sensitivity to the previously suggested 10 bpm HRV limit for prospective CCTA. What follows is a description of the scanner's architecture, including general comments applicable to prospective wide-area detector scanning.

Detector coverage

The ability to cover the cardiac anatomy in two axial acquisitions (Fig. 1) is enabled by detector coverage of 80 mm (128 $\times$ 0.625 mm) and dynamic z-focal spot (ZFS), resulting in a sampled collimation of 256 simultaneous slices. As the cone beam geometry of the large coverage system requires overlap between adjacent axial slices [13], craniocaudal coverage of 124.8 mm can be covered with two axial acquisitions each with X-ray exposure during a rest phase of two heart beats and one beat between used for translating the patient couch. As noted by Hsieh et al., the overlap between adjacent axial acquisitions is dependent on the planned transaxial FOV [13]. The two-shot coverage of 124.8 mm provides reconstruction at a full FOV up to 250 mm. However, reducing the FOV to 200 mm, as appropriate in a vast majority of coronary CTA exams, enables craniocaudal coverage up to 132.0 mm to be reconstructed without data truncation or associated extrapolation artifacts [13]. To achieve craniocaudal coverage of 140 mm, image volumes can be reconstructed at full FOV up to 143 mm. While this FOV is likely sufficient for pediatric and small patient populations, an additional axial acquisition will extend the craniocaudal coverage for larger fields of view. Given the discrete nature of prospective axial imaging, three axial shots for a full 250 mm FOV would result in craniocaudal coverage of 187.4 mm. If only 140 mm of coverage were desired, a z-overscan of 47.4 mm (33.9%) would result. To mitigate this decrease in dose efficiency, the system automatically chooses an optimal detector collimation to (1) minimize the number of steps and (2) reduce the amount of z-overscan. Furthermore, to image the entire cardiac anatomy from the top of the aortic arch to the apex of the heart, 150–190 mm of craniocaudal coverage is typically necessary. At the upper end of this range, the anatomy is covered without z-overscan using just three axial acquisitions at a full cardiac field of view. Lastly, all prospective CCTA images using 256-slice MDCT are reconstructed with dedicated three-dimensional axial reconstruction algorithms to eliminate cone-beam artifacts often associated with large detector coverage [37].

The reduction in the number of axial shots required to cover the necessary cardiac anatomy using 256-slice MDCT with 80 mm detector coverage is a significant improvement compared to the previous results reported in 64-slice and dual-source MDCT studies [14–21]. While still requiring a single step when imaging anatomy greater than 80 mm in length, the resulting transition zone and potential for stair-step artifact has not been associated with non-diagnostic images as noted in previous studies with 40.0 mm of detector coverage [14, 16–18, 20]. Should stair-step artifacts arise, unlike the 64-slice and dual-source systems—where such artifacts between the first and second axial shot are likely to fall in the proximal segments of the coronary arteries—the 80 mm

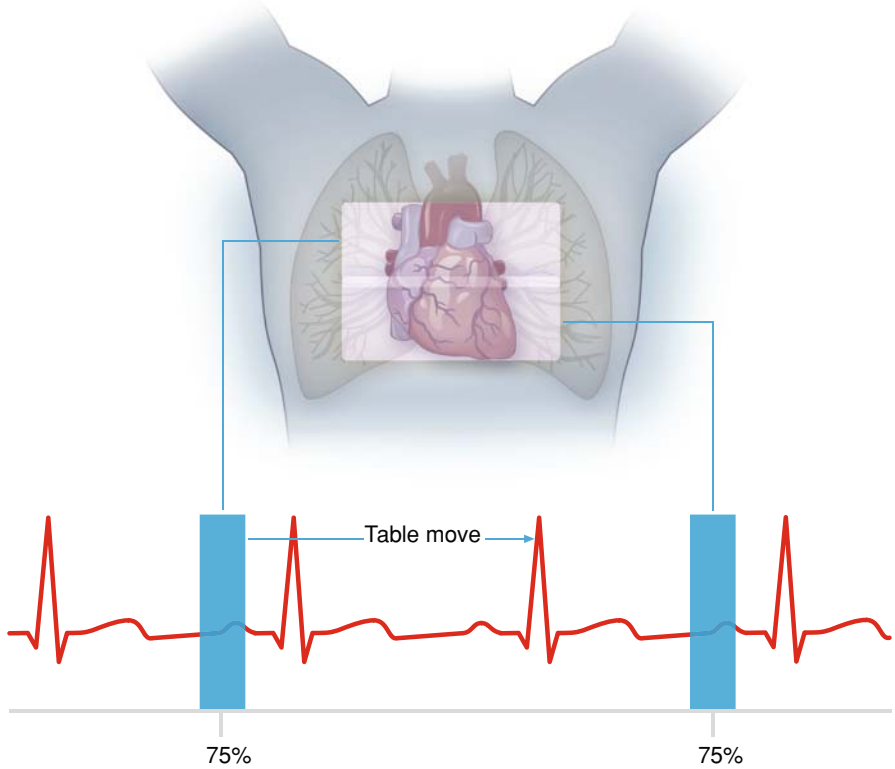

Fig. 1 Prospectively gated axial coronary CTA using two axial acquisitions (shots) with 2 × 128 × 0.625 mm detector collimation and dynamic z-focal spot to cover the relevant cardiac anatomy from the level of the carina to the apex. Using a prospective ECG trigger, typically in mid-diastole at 75% of the R-R interval, the first X-ray acquisition of 80 mm occurs during a small portion of one cardiac cycle while the patient couch is stationary. After the first shot is complete, the X-rays are turned off and the patient couch is translated 62.4 mm to the next axial location. A second 80 mm axial acquisition at the next craniocaudal location is then performed during the next cardiac cycle. The amount of overlap between axial acquisitions is linearly related to the planned transaxial field of view (FOV), with a smaller FOV reducing the amount of overlap. The overlapping regions are necessary to prevent data truncation (and the need for extrapolation) in the dedicated three-dimensional axial algorithms used to reconstruct data from large coverage detectors

coverage would shift any such artifacts toward the mid or distal segments. Furthermore, when the scan length is greater than 160—as needed for coronary artery bypass grafts (CABG) and great vessels—the aforementioned automatic collimation selection prevents the z-overscan that would otherwise be associated with such multiple axial acquisitions.

In addition to reducing the number of axial shots necessary to cover the cardiac anatomy compared to previous generation scanners, the wider coverage 256-slice MDCT enables a substantial reduction in scan durations. Typical scan durations for prospective CCTA with 256-slice MDCT are approximately 2.1 and 3.9 s, respectively, for a 70 and 60 bpm scan with two axial acquisitions. These short scan times facilitate a reduction in the contrast volume needed for opacification of the relevant cardiac anatomy. Based on the above scan times and previously reported contrast protocols [14, 16], 50 ml of iodinated contrast should be appropriate for patients with normal cardiac output. This is a 40–60% reduction in contrast compared to previous studies [15, 17, 18, 20, 22]. This reduces the risk of contrast induced nephropathy and may indicate a potential for institutional cost reduction.

Moreover, shorter scan times associated with larger detector coverage of 256-slice MDCT lead to less susceptibility to sinus arrhythmia (HRV) and

ectopic beats. This reduced susceptibility to HRV results from the reduced time in which the HR can change during the scan (e.g., as associated with Valsalva response). Contrarily, the opportunity for ectopy during an acquisition is significantly reduced with a fewer number of cardiac cycles required. Scan times with 256-slice MDCT are substantially shorter than previous studies, particularly those performed with dual-source MDCT that have reported mean scan durations of 14–15 s [19, 21]. This 72–85% reduction in scan time clearly reduces the opportunity for HRV and/or ectopy. Less significant, yet still important, scan duration reductions of approximately 50% are possible compared to 64-slice MDCT [14, 16–18, 20]. Similar to the technology reported by Klass et al., the 256-slice scanner incorporates real-time arrhythmia management capability that enables the X-ray acquisition to be paused upon the detection of ectopy and resumed at the same axial location once normal sinus rhythm has returned [18]. It is interesting to note that shorter scan times associated with large coverage scanners enable longer pauses to allow for the management of multiple or complex arrhythmias without sacrificing contrast timing.

Temporal resolution and prospective triggering

The ability to image patients with higher heart rates using prospective CCTA is enabled by a 0.27 s gantry rotation time on 256-slice MDCT. This gantry rotation time results in a standard single cycle temporal resolution of 135 msec, thus enabling patients to be imaged in mid-diastole, with heart rates up to 75 bpm, the physiologic limit of diastasis for most patients. Additionally, the 135 ms temporal resolution permits prospective imaging at the end-systolic rest period for patients with heart rates above 75 bpm (Fig. 2). The flexibility to image in either rest period makes possible the patient-specific selection of imaging windows based on heart rate. The default scan cycle provides ±15 ms of X-ray padding that enables a variable delay algorithm (Beat-to-Beat, Philips Healthcare, Cleveland, OH, USA) to automatically adjust the reconstruction window within this buffer to track diastasis in the presence of heart rate variation [38, 39]. Should extreme HRV be expected prior to CCTA, additional phase tolerance of ±75 ms may be added on an as-needed basis (Fig 2). This additional padding may be particularly important when imaging in the end-systolic rest period, given the relatively short rest period duration compared to the single cycle temporal resolution and the proximity to the adjacent rapid ejection and rapid filling phases. Novel QRS detection algorithms have also been introduced to improve accuracy and reduce sensitivity to noise. These improvements, in combination with the variable delay algorithm, facilitate accurate prediction of mid-diastolic and end-systolic imaging windows that are optimally aligned with cardiac rest periods based on local statistical combinations of the previous one to five R-R intervals.

X-Ray tube power

The ability to image obese and bariatric patients with BMI greater than 30 kg/m^2 using prospective CCTA requires higher X-ray tube power (e.g., 120 kW) and noise-reduction measures [40, 41]. A 120 kW system provides the necessary instantaneous tube power to support 0.27 s rotation times in a prospective acquisition mode. For a given tube voltage, higher tube currents of up to 1,000 mA ensure sufficient photon flux necessary for diagnostic signal to noise ratio (SNR) in obese and bariatric patients. Noise reduction can be accomplished by the use of a post-patient, detector-mounted, two-dimensional anti-scatter grid (2D ASG). Such a 2D ASG reduces scatter by a factor of three [40, 41] compared to a traditional one-dimensional ASG. This improvement in scatter-to-primary ratio (SPR) increases CT number homogeneity in the bariatric thorax and facilitates an increase in low contrast resolution for soft tissue imaging [40, 41], which is particularly important for characterizing non-calcified plaque and regions of reduced myocardial perfusion in all patients. In addition to providing the X-ray tube power necessary to image obese patients, increased tube current-time products (mAs) are possible at reduced tube voltages (e.g., 80 kVp) such that diagnostic image quality at substantially reduced effective radiation dose is possible in small- and medium-sized patients [24].

256-Slice MDCT prospectively gated axial coronary in clincal practice

Since May 2008, we have performed prospective CCTA (Step & Shoot Cardiac, Philips Healthcare,

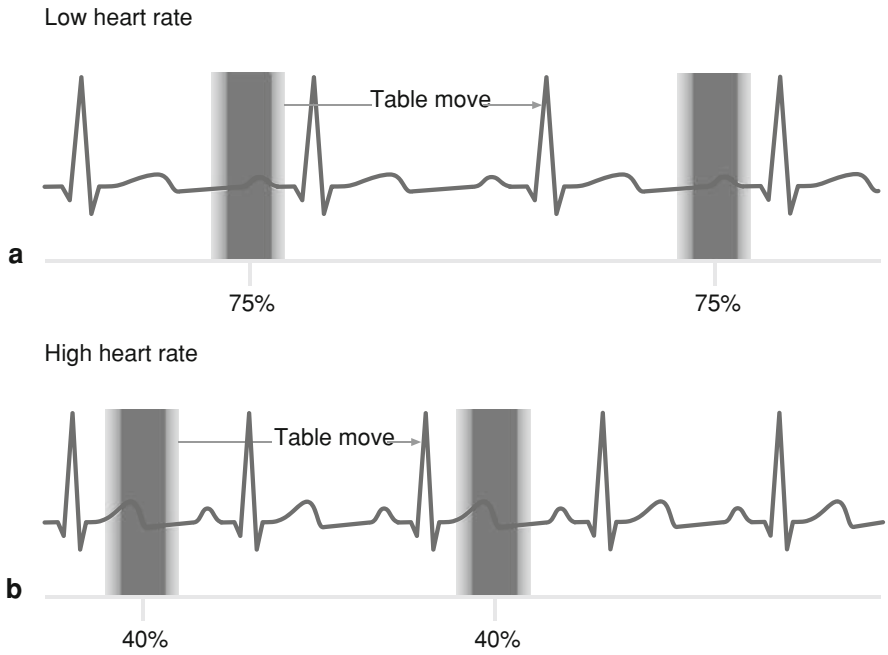

Fig. 2 For patients with low heart rates (≤75 bpm), a mid-diastolic trigger centered at 75% of the R-R interval (**a**) is used to align the imaging window with diastasis. At high heart rates (>75 bpm), an end-systolic imaging window centered at 40% of the R-R interval (**b**) is used to image the heart in a rest period composed of the reduced ejection, protodiastole, and isovolumetric relaxation time phases. The minimum X-ray acquisition window necessary for reconstruction (*dark grey rectangles*) results in a standard single cycle temporal resolution of 135 ms for a gantry rotation time of 0.27 s. Additional X-ray padding (*light grey rectangles*) of ±15 to ±90 ms can be added to reconstruct additional phases around the prospectively triggered phase

Cleveland, OH, USA) with 256-slice MDCT in our clinical practice on over 400 patients. Unlike our 64-slice MDCT, where we instituted a clinical algorithm similar to that described by Earls et al. [23], we have completely changed our clinical algorithm to heavily favor using prospective gating to image patients referred for coronary CTA (Fig. 3). Nearly 100% of patients are scanned with the prospective protocol, unless reconstructed phases throughout the cardiac cycle are needed for assessment of left ventricular function or for preoperative assessment of the proximity of bypass grafts to the midsternal line. If reconstructed images are needed across the complete cardiac cycle, we use a retrospective protocol, with or without ECG-triggered dose modulation, depending on clinical indication.

We use a prospective protocol in patients for whom only a single cardiac phase is needed for coronary assessment. We typically use a tube voltage of 120 kVp and a tube current-time product between 200 and 360 mAs, adjusting primarily the mAs based on body habitus. We typically inject 50–60 ml of iodinated contrast (Isovue 370, Bracco Diagnostics, Princeton, NJ, USA) at a flow rate of 5 ml/s, followed by a 40 ml bolus of saline at the same rate using a dual-head injector (Stellant D, Medrad, Warrendale, PA, USA). We trigger our scan using an automatic bolus tracking technique, with a region of interest (ROI) placed in the main pulmonary artery and a threshold of 175 HU. This is an unusual location for a trigger ROI—one which requires taking pulmonary circulation time into account; however, using a post-threshold delay of 10–12 s, we have found good results in terms of coronary opacification. To save time and increase patient throughput, we do not routinely administer β blocker medications, unless the patient's heart rate is greater than 80 bpm prior to CCTA. In those patients, we administer 5–15 mg of intravenous metoprolol after the scout scans are performed. Each patient receives 400 to 800 mcg of sublingual nitroglycerin immediately before CCTA. For all patients with a prescan HR of less than or equal to 75 bpm, we use a mid-diastolic trigger centered at 75% of the R-R interval and for patients

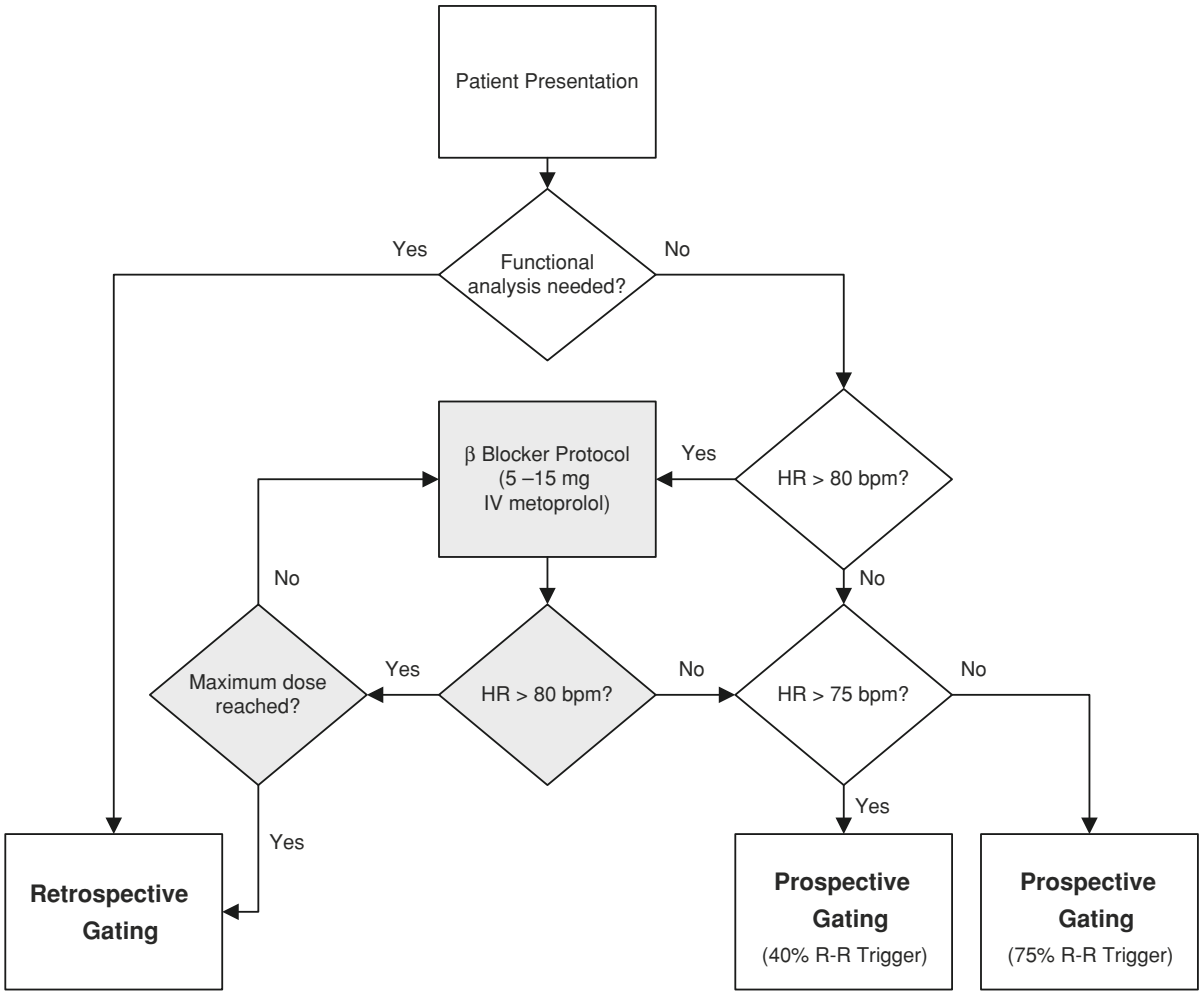

Fig. 3 Clinical algorithm for selecting prospective or retrospective CCTA. A prospectively gated technique is applied in all patients not requiring multiphase reconstructions for functional analysis. Unless the patient has pre-scan heart rate (HR) greater than 80 bpm, no β blocker medications are given. All prospectively-gated acquisitions in patients with HR $\leq$75 bpm are imaged with a mid-diastolic trigger, whereas patients with HR >75 bpm are imaged with an end-systolic trigger

with a prescan HR greater than 75 bpm, we trigger the scan at an end-systolic trigger of 40% of the R-R interval. We also factor in an expected 5–10 bpm drop in HR that typically occurs subsequent to breathhold. In our experience, this is an optimal time to image due to the short scan time associated with the 256-slice scanner. Since this is both our initial experience with a new 256-slice MDCT scanner and a significant change to our clinical algorithm (e.g., performing CCTA routinely without β blocker medication, and using prospective gating for patients with HR >75 bpm), we routinely apply $\pm$75 ms of padding in prospective mode to provide conservative imaging windows. In the future, we plan to make patient-specific padding decisions based on both prescan HR and HRV [36]. Additionally, like our 64-channel MDCT system, our 256-slice MDCT scanner has the ability to manage ectopic beats through real-time arrhythmia detection and system response.

Based on a randomly selected population sample of 89 patients (77 prospective and 12 retrospective CCTA) from June 2008 through September 2008—our first four full months using our 256-slice MDCT scanner, we have calculated mean effective radiation dose as the product of the scanner-reported

dose-length product (DLP) and a gender & body-habitus averaged conversion coefficient, $k = 0.014$ mSv·mGy^{-1}·cm^{-1}, for the adult thorax [42, 43]. In this way, we realized a mean (±SD) effective radiation dose of 4.0 ± 1.0 mSv (range, 2.1–7.0 mSv) for prospective CCTA. A comparative cohort of 12 retrospective CCTA cases resulted in a mean effective radiation dose of 11.4 ± 3.4 mSv (range, 6.0–17.6 mSv), noting that 9 (75%) of patients had ECG-triggered dose modulation applied for mean dose reduction of 36.1 ± 6.8% (range, 19.2–44.7%). Comparatively, prospective acquisition conferred a mean dose reduction of 64.6% compared to traditional, retrospective CCTA. The mean heart rate immediate prior to prospective CCTA was 70.1 ± 12.7 bpm (range, 42.0–102.0 bpm), with a mean heart rate of 66.2 ± 14.1 bpm (range, 43.0–116.0 bpm) during prospective CCTA. Twenty-four patients (31.2%) had an initial HR greater than 75 bpm, with 16/24 (66.7%) of those patients above 80 bpm prior to prospective acquisition. However, during prospective CCTA, 20 of 77 (26.0%) and 15 of 20 (75.0%) patients had heart rates above 75 and 80 bpm, respectively, with the HR reduction likely attributed to breathhold. With respect to prospective trigger selection, 49 of 77 (63.6%) and 28 of 77 (36.4%) patients were acquired with mid-diastolic and end-systolic imaging windows, respectively. In patients with a pre-scan HR greater than 75 bpm, 22 of 35 (62.9%) were imaged using an end-systolic trigger. The remaining 6 patients in whom a 40% prospective trigger was used had pre-scan heart rates just below 75 bpm. HRV during prospective scanning was 2.0 ± 3.1 bpm (range, 0.0–21.5 bpm). The mean craniocaudal coverage was 129.8 ± 15.0 mm (range, 109.2–187.2 mm), requiring two axial acquisitions in 65 of 77 (84.4%) and three axial acquisitions in 12 of 77 (15.4%) patients. Mean scan duration was 4.5 ± 0.9 s (range, 3.6–8.2 s), including the additional padding applied to each axial acquisition, and was longest for patients with lower heart rates and three axial acquisitions. It is interesting to note that our mean transaxial FOV reconstructed from prospective CCTA was 175.4 ± 25.3 mm (range, 133.0–278.0 mm), with 76 of 77 (98.7%) of patients having a reconstructed FOV less than 250 mm. This suggests that additional patients could be scanned with two—instead of three—axial acquisitions by more judicious planning on the anteroposterior (AP) scout image. In this randomly selected cohort, all patients were scanned with a 0.27 s rotation time, a tube voltage of 120 kVp, and a mean tube current-time product of 240.5 ± 57.8 mAs (range, 150–360 mAs).

While larger studies are necessary to determine the effect of heart rate and prospective trigger selection on image quality, we show four representative cases using prospectively gated 256-slice MDCT that span a range of heart rates from 60–90 bpm. Using our patient selection algorithm, the above described scan and contrast protocols were applied in these four cases. The first representative patient (Fig. 4a, b) was a 53 year old male who presented with atypical chest discomfort and a small mild distal anterior perfusion defect on his exercise SPECT. His mean initial prescan HR was 68 bpm, so no β blocker medication was administered, resulting in a mean (±SD) HR of 63 ± 0.8 bpm during CCTA. He was scanned with prospective gating using a mid-diastolic trigger at 75% of the R-R interval. A craniocaudal coverage of 124.8 mm was scanned in 3.9 s using two axial acquisitions with a 2 × 128 × 0.625 mm (80 mm) detector collimation including ZFS at a gantry rotation time of 0.27 s. An X-ray technique of 120 kVp, 250 mAs, and ±70 ms of padding, resulted in an effective dose of 4.2 mSv. A 45 ml bolus of 370 mgI/ml contrast was injected intravenously at 5 ml/s followed by a 40 ml saline bolus. Images were reconstructed with a semi-sharp reconstruction kernel (XCC) at an FOV of 171 mm using a slice thickness of 0.9 mm with 50% overlap. The CCTA reveals an anomalous RCA arising from the left coronary sinus, but no coronary stenosis. The absence of perfusion defect in the RCA territory frees the anomalous coronary from implication as a cause of the patient's symptoms.

A second example case (Fig. 4c, d) was from a 57 year old male that was indicated for CCTA because of atypical chest discomfort. Without β blocker medication, he had a mean heart rate 70 ± 0.5 bpm during prospective CCTA and was scanned with a mid-diastolic trigger at 75% of the R-R interval. A 2 × 128 × 0.625 mm (80 mm) detector collimation resulted in a scan length of 124.8 mm using two axial shots. A tube voltage of 120 kVp, a tube current-time product of 360 mAs, including ±90 ms of padding yielded an effective radiation dose of 5.1 mSv. The contrast protocol was identical to the first patient. Reconstructed images at an FOV of 210 mm and a slice thickness of 0.9 mm using a semi-smooth (XCB) reconstruction filter were generated. CCTA reveals

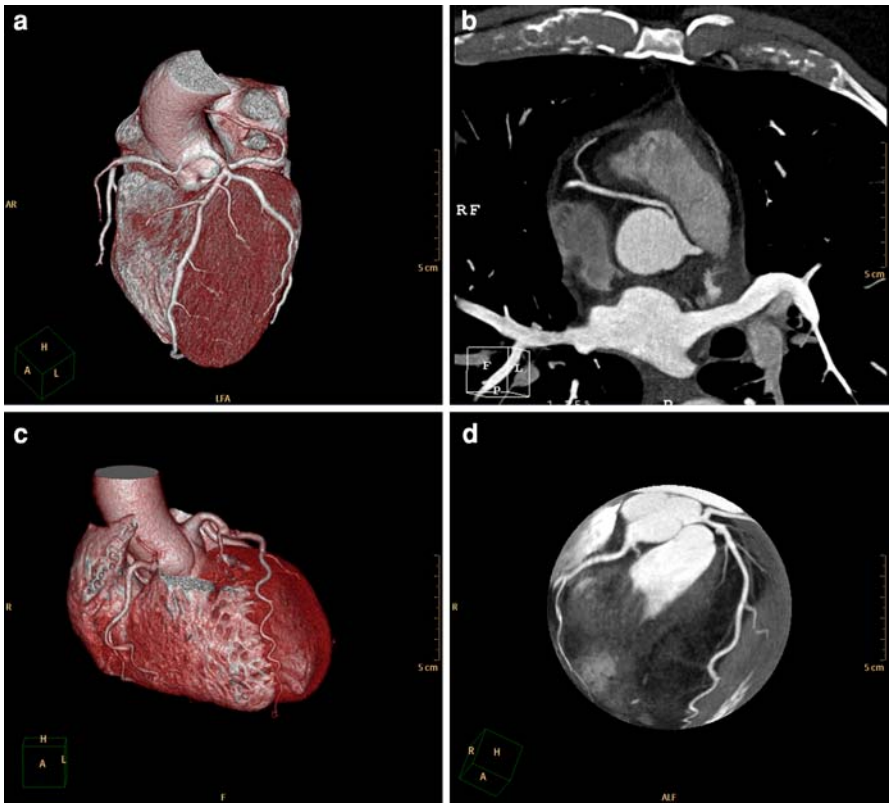

Fig. 4 Prospectively gated **a** volume-rendered and **b** slab maximum intensity projection (MIP) images of a 53 year old male who presented with atypical chest discomfort and a small mild distal anterior perfusion defect on his exercise SPECT. The patient was scanned without β blocker medication using a mid-diastolic trigger at 75% of the R-R. Mean HR and effective radiation dose at CCTA were 63 ± 0.8 bpm and 4.2 mSv, respectively. The CCTA reveals an anomalous RCA, but no coronary stenosis. Representative case with **c** volume-rendered and **d** globe MIP images of a 57 year old scanned with prospective gating at mean heart rate of 70 ± 0.5 bpm also using a mid-diastolic trigger at 75% of the R-R interval. Effective radiation dose of prospective CCTA was 5.1 mSv. The CCTA reveals small coronary calcifications but no significant coronary stenosis

small coronary calcifications but no significant coronary stenosis.

Two patients with heart rates above 75 bpm were scanned using an end-systolic trigger at 40% of the R-R interval without pharmacologic HR control. The third patient (Fig. 5a, b) was a 59 year old male presenting with a single episode of chest burning lasting approximately 5 min. A pre-scan HR of 79 bpm rose slightly to 81 ± 0.9 bpm during acquisition. Scan and contrast protocols were identical to the first two patients, with the exception of the tube current-time product and X-ray padding, which were 325 mAs (adjusted for body habitus) and ±70 ms, respectively. The resulting scan time was 4.2 s and images were reconstructed using a semi-sharp filter (XCC) at a transaxial FOV of 200 mm and a slice thickness of 0.9 mm. Effective radiation dose at CCTA was 5.5 mSv. CCTA was able to demonstrate that while a small amount of coronary plaque was present, no severe stenosis was present.

A fourth representative case comes from a 59 year old female patient (Fig. 5c, d). The clinical indication for CCTA was sharp chest pain. She had a mean heart rate and heart rate variation of 92 and 1.6 bpm, respectively, during prospective acquisition triggered at 40% of the R-R interval. Each axial shot used an additional ±70 ms of padding at 200 mAs. All other scan and contrast parameters were similar to the previously described cases, with minor differences in FOV, which was 162 mm. The resulting effective dose was 2.8 mSv. CCTA revealed that she had no coronary artery disease.

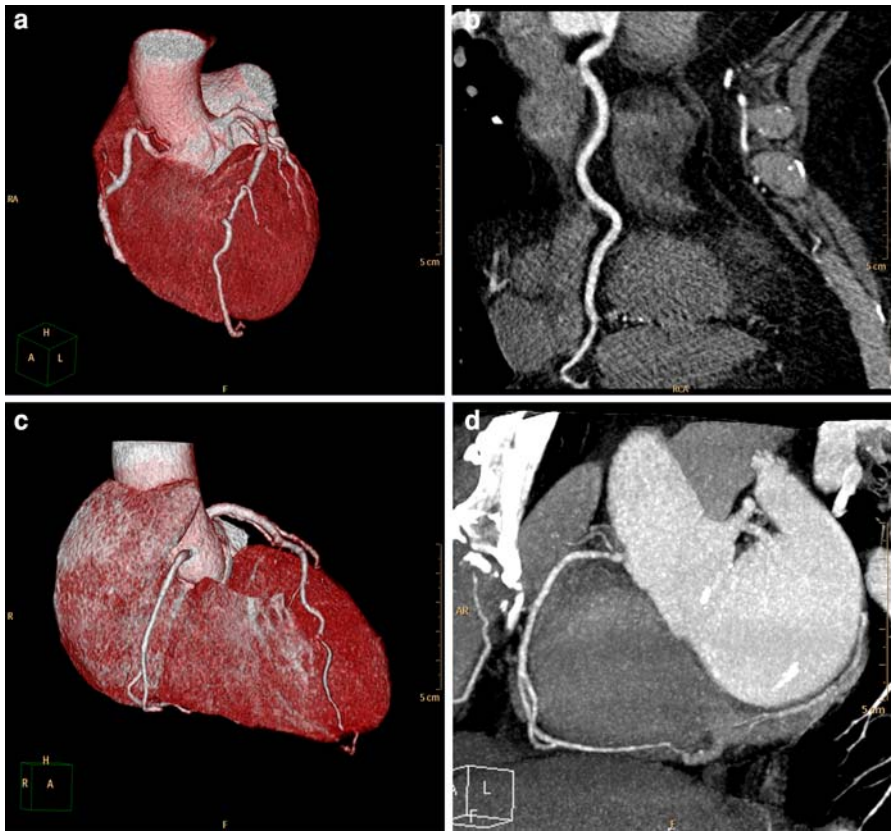

Fig. 5 Two patients with heart rates above 75 bpm were scanned using an end-systolic trigger at 40% of the R-R interval without pharmacological HR control. **a** Volume-rendered and **b** curved multiplanar reformatted (cMPR) images of a 59 year old male indicated for CCTA because of chest burning. Mean HR and effective dose of prospective CCTA were 81 ± 0.9 bpm and 5.5 mSv, respectively. The CCTA reveals a small amount of coronary plaque but no severe stenosis. At a mean heart rate and heart rate variation of 92 and 1.6 bpm, respectively, **c** volume-rendered and **d** slab MIP images of a 59 year old female patient. The clinical indication for CCTA was sharp chest pain. Resulting effective dose was 2.8 mSv. The CCTA demonstrates no coronary artery disease

Conclusions

While large scale studies are necessary, the technical advances of and early clinical results from 256-slice MDCT indicate that high-quality, low-dose prospective coronary CTA can be applied in patients with higher heart rates, higher BMI, and with less sensitivity to heart rate variability. Additionally, concomitant reduction in intravenous contrast and imaging without β blocker medication may be possible. In conclusion, 256-slice MDCT may enable the application of low-dose prospective coronary CTA in a wider range of patients compared to prior generations of MDCT.

Acknowledgments The authors would like to thank Ronda Bruce for her assistance in the creation of clinical figures and Scott Pohlman, Mani Vembar, and Thomas Ivanc for their contributions in reviewing this paper. Additionally, the authors acknowledge the Washington Hospital Center cardiac CT technologists and nurse for their daily dedication and support.

Conflict of interest Authors who are not employees of Philips Healthcare (Cleveland, OH, USA) controlled the inclusion of all data and information that might have represented a conflict of interest for the authors who are employees of that company.

References

1. Phurrough SE, Salive ME, Baldwin J et al (2008) Decision memo for computed tomographic angiography (CAG-00385 N). In: Medicare national coverage determinations manual. Sect. 220.1F. CMS publication 100-03. Centers for Medicare & Medicaid Services. http://www.cms.hhs.gov/mcd/viewdecisionmemo.asp?id=206. Accessed December 7, 2008
2. Brenner DJ, Hall EJ (2007) Computed tomography—an increasing source of radiation exposure. N Engl J Med 357:2277–2284. doi:10.1056/NEJMra072149
3. Budoff MJ, Achenbach S, Blumenthal RS et al (2006) Assessment of coronary artery disease by cardiac computed tomography: a scientific statement from the American heart association committee on cardiovascular imaging and intervention, Council on cardiovascular radiology and intervention, and Committee on cardiac imaging, Council on clinical cardiology. Circulation 114:1761–1791. doi:10.1161/CIRCULATIONAHA.106.178458
4. Einstein AJ, Moser KW, Thompson RC et al (2007) Radiation dose to patients from cardiac diagnostic imaging.

Circulation 116:1290–1305. doi:10.1161/CIRCULATIONAHA.107.688101
5. Paul JF, Abada HT (2007) Strategies for reduction of radiation dose in cardiac multislice CT. Eur Radiol 17:2028–2037. doi:10.1007/s00330-007-0584-3
6. Hausleiter J, Meyer T (2008) Tips to minimize radiation exposure. J Cardiovasc Comput Tomogr 2:325–327. doi:10.1016/j.jcct.2008.08.012
7. Hausleiter J, Meyer T, Hadamitzky M et al (2006) Radiation dose estimates from cardiac multislice computed tomography in daily practice: impact of different scanning protocols on effective dose estimates. Circulation 113:1305–1310. doi:10.1161/CIRCULATIONAHA.105.602490
8. Leschka S, Stolzmann P, Schmid FT et al (2008) Low kilovoltage cardiac dual-source CT: attenuation, noise, and radiation dose. Eur Radiol 18:1809–1817. doi:10.1007/s00330-008-0966-1
9. Halliburton SS (2008) One-scan protocol does not fit all: responsible cardiovascular imaging with computed tomography. J Cardiovasc Comput Tomogr 2:323–324. doi:10.1016/j.jcct.2008.08.009
10. Gutstein A, Dey D, Cheng V et al (2008) Algorithm for radiation dose reduction with helical dual source coronary computed tomography angiography in clinical practice. J Cardiovasc Comput Tomogr 2:311–322. doi:10.1016/j.jcct.2008.07.003
11. Coles DR, Smail MA, Negus IS et al (2006) Comparison of radiation doses from multislice computed tomography coronary angiography and conventional diagnostic angiography. J Am Coll Cardiol 47:1840–1845. doi:10.1016/j.jacc.2005.11.078
12. Mollet NR, Cademartiri F, van Mieghem CAG et al (2005) High-resolution spiral computed tomography coronary angiography in patients referred for diagnostic conventional coronary angiography. Circulation 112:2318–2323. doi:10.1161/CIRCULATIONAHA.105.533471
13. Hsieh J, Londt J, Vass M et al (2006) Step-and-shoot data acquisition and reconstruction for cardiac X-ray computed tomography. Med Phys 33:4236–4248. doi:10.1118/1.2361078
14. Earls JP, Berman EL, Urban BA et al (2008) Prospectively gated transverse coronary CT angiography versus retrospectively gated helical technique: improved image quality and reduced radiation dose. Radiology 246:742–753. doi:10.1148/radiol.2463070989
15. Gutstein A, Wolak A, Lee C et al (2008) Predicting success of prospective and retrospective gating with dual-source coronary computed tomography angiography: development of selection criteria and initial experience. J Cardiovasc Comput Tomogr 2:81–90
16. Hirai N, Horiguchi J, Fujioka C et al (2008) Prospective versus retrospective ECG-gated 64-detector coronary CT angiography: assessment of image quality, stenosis, and radiation dose. Radiology 248:424–430. doi:10.1148/radiol.2482071804
17. Husmann L, Valenta I, Gaemperli O et al (2008) Feasibility of low-dose coronary CT angiography: first experience with prospective ECG-gating. Eur Heart J 29:191–197. doi:10.1093/eurheartj/ehm613
18. Klass O, Jeltsch M, Feuerlein S et al (2008) Prospectively gated axial CT coronary angiography: preliminary experiences with a novel low-dose technique. Eur Radiol. doi:10.1007/s00330-008-1222-4
19. Scheffel H, Alkadhi H, Leschka S et al (2008) Low-dose CT coronary angiography in the step-and-shoot mode: diagnostic performance. Heart 94:1132–1137. doi:10.1136/hrt.2008.149971
20. Shuman WP, Branch KR, May JM et al (2008) Prospective versus retrospective ECG gating for 64-detector CT of the coronary arteries: comparison of image quality and patient radiation dose. Radiology 248:431–437. doi:10.1148/radiol.2482072192
21. Stolzmann P, Leschka S, Scheffel H et al (2008) Dual-source CT in step-and-shoot mode: noninvasive coronary angiography with low radiation dose. Radiology 249:71–80. doi:10.1148/radiol.2483072032
22. Rybicki FJ, Otero HJ, Steigner ML et al (2008) Initial evaluation of coronary images from 320-detector row computed tomography. Int J Cardiovasc Imaging 24:535–546. doi:10.1007/s10554-008-9308-2
23. Earls JP (2008) Questions in cardiovascular CT: how to use a prospective gated technique for cardiac CT. J Cardiovasc Comput Tomogr 3(1):45–51. doi:10.1016/j.jcct.2008.10.013
24. Nakayama Y, Awai K, Funama Y et al (2005) Abdominal CT with low tube voltage: preliminary observations about radiation dose, contrast enhancement, image quality, and noise. Radiology 237:945–951. doi:10.1148/radiol.2373041655
25. Arevalo F, Sakamoto T (1964) On the duration of the isovolumetric relaxation period (IVRP) in dog and man. Am Heart J 67:651–656. doi:10.1016/0002-8703(64)90336-9
26. Luisada AA, MacCanon DM (1972) The phases of the cardiac cycle. Am Heart J 83:705–711. doi:10.1016/0002-8703(72)90412-7
27. Wiggers CJ (1921) Studies on the consecutive phases of the cardiac cycle. The duration of the consecutive phases of the cardiac cycle and the criteria for their precise determination. Am J Physiol 56:415–438
28. Wiggers CJ (1921) Studies on the consecutive phases of the cardiac cycle. The laws governing the relative durations of ventricular systole and diastole. Am J Physiol 56:439–459
29. Chung CS, Karamanoglu M, Kovács SJ (2004) Duration of diastole and its phases as a function of heart rate during supine bicycle exercise. Am J Physiol Heart Circ Physiol 287:H2003–H2008. doi:10.1152/ajpheart.00404.2004
30. Wang Y, Vidan E, Bergman GW (1999) Cardiac motion of coronary arteries: variability in the rest period and implications for coronary MR angiography. Radiology 213:751–758
31. Herzog C, Abolmaali N, Balzer JO et al (2002) Heart-rate-adapted image reconstruction in multidetector-row cardiac CT: influence of physiological and technical prerequisite on image quality. Eur Radiol 12:2670–2678
32. Bahler RC, Vrobel TR, Martin P (1983) The relation of heart rate and shortening fraction to echocardiographic indexes of left ventricular relaxation in normal subjects. J Am Coll Cardiol 2:926–933
33. Weissler AM, Harris WS, Schoenfeld CD (1968) Systolic time intervals in heart failure in man. Circulation 37:149–159

34. Stafford RW, Harris WS, Weissler AM (1970) Left ventricular systolic time intervals as indices of postural circulatory stress in man. Circulation 41:485–492
35. Manzke R, Grass M, Nielsen T et al (2003) Adaptive temporal resolution optimization in helical cardiac cone beam CT reconstruction. Med Phys 30:3072–3080. doi:10.1118/1.1624756
36. Steigner ML, Otero HJ, Cai T et al (2009) Narrowing the phase window width in prospectively ECG-gated single heart beat 320-detector row coronary CT angiography. Int J Cardiovasc Imaging 25:85–90. doi:10.1007/s10554-008-9347-8
37. Köhler TH, Proksa R, Grass M (2001) A fast and efficient method for sequential cone-beam tomography. Med Phys 28:2318–2327. doi:10.1118/1.1395025
38. Heuscher DJ, Chandra S (2003) Multi-phase cardiac imager. US Patent 6510337
39. Vembar M, Garcia MJ, Heuscher DJ et al (2003) A dynamic approach to identifying desired physiological phases for cardiac imaging using multislice spiral CT. Med Phys 30:1683–1693. doi:10.1118/1.1582812
40. Engel KJ, Bäumer C, Wiegert J et al (2008) Spectral analysis of scattered radiation in CT. In: Hsieh J, Samei E (eds) Medical imaging 2008: physics of medical imaging 6913:69131R. Society of Photographic Instrumentation Engineers, Bellingham, Washington, USA
41. Vogtmeier G, Dorscheid R, Engel KJ et al (2008) Two-dimensional anti-scatter-grids for computed tomography detectors. In: Hsieh J, Samei E (eds) Medical imaging 2008: physics of medical imaging 6913:69159R. Society of Photographic Instrumentation Engineers, Bellingham, Washington, USA
42. McCollough C, Cody D, Edyvean S, et al (2008) The measurement, reporting, and management of radiation dose in CT. Technical report 96, American Association of Physicists in Medicine, College Park, MA, USA
43. Shrimpton PC (2004) Assessment of patient dose in CT. Technical report NRPB-PE/1/2004, National Radiological Protection Board, Chilton, UK